

15. DATA REPORT: SITE 918 IRD MASS ACCUMULATION RATE RECORD, LATE MIOCENE–PLEISTOCENE¹

Kristen E. Kudless St. John²

INTRODUCTION

To understand the late Cenozoic glacial history of the Northern Hemisphere, continuous long-term proxy records from climatically sensitive regions must be examined. Ice-rafted debris (IRD) from Ocean Drilling Program (ODP) Site 918, located in the Irminger Basin, is one such record. IRD in marine sediments is a direct indicator of the presence of glacial ice extending to sea level on adjacent landmasses, and, therefore, is an important paleoclimatic signal from the mid- to high latitudes. The IRD record at Site 918 is the first long-term ice-rafting record available for southeast Greenland, a region that may have been a key nucleation area for widespread glaciation during the late Cenozoic (Larsen et al., 1994). This data report presents the results of coarse sand-size IRD mass accumulation rate (MAR) analyses for Site 918 from the late Miocene through the Pleistocene. In addition, a preliminary analysis of IRD compositions is included. Detailed discussions of the local, regional, and global paleoclimatic implications of this data, and of the companion Site 919 Pleistocene IRD MAR data (Krissek, Chap. 14, this volume), are in preparation. Such future work will include comparisons of these IRD MAR data sets to the Site 919 oxygen isotope stratigraphy developed by Flower (1998).

MATERIALS AND METHODS

Samples 10 to 20 cm³ in volume were taken at a spacing of approximately every 50 to 75 cm from the upper Miocene to Holocene sediments of Holes 918A and 918D. Variations in sample spacing reflect changes in core recovery and the effort to avoid coarse-grained turbidite and ash layers during sampling. Five hundred eighteen samples were analyzed. The sedimentation rates used to calculate sample ages were determined by using available postcruise magnetostratigraphic (Fukuma, 1998) and biostratigraphic (Spezzaferri, 1998; Wei, 1998) age-depth data. Note that the Pliocene/Pleistocene transition, between ~1.4 and ~1.7 Ma, is expressed as a hiatus of ~300 k.y. The time averaged within individual samples typically ranges from 0.1 k.y. to 1.0 k.y., depending on the particular sample volume and sedimentation rate. Such time averaging is on a considerably finer scale than the temporal resolution of the IRD MAR variations presented in this study (i.e., averaging ~12 k.y.), and, therefore, does not significantly affect the IRD MAR results or paleoclimatic conclusions drawn from these results.

Complete descriptions of the lithologic units sampled are given in Shipboard Scientific Party (1994); therefore, only a brief summary of the lithologies follows. Nearly all the samples for this study are taken

from lithologic Unit I, which extends from 0.0 to 600.0 meters below seafloor (mbsf) and is dominated by a dark gray silt of Holocene to late Miocene age. It is divided into five subunits, based on the presence of graded beds in the upper two subunits and on the downcore decrease in IRD in the lower three subunits. Subunit IC is noted to contain the highest concentration of IRD in Unit I. The last occurrence of an unequivocal in situ dropstone is at 543.6 mbsf, marking the base of Subunit ID. No dropstones were observed in Subunit IE during the shipboard description. The oldest sediments sampled for this study are dated as late Miocene (~8.7 Ma) and were taken from the upper 2 m of lithologic Unit II, which is composed of a moderately to heavily bioturbated nannofossil chalk and silt.

Previous studies in the Norwegian-Greenland Sea (Krissek, 1989) and North Pacific (von Huene et al., 1973, 1976; Krissek et al., 1985; Krissek, 1995) have shown that the 250 µm–2 mm grain-size interval is a valid indicator of IRD abundance, and the coarse-sand abundance is interpreted in a similar fashion in this study. Samples were dried at 60°C, weighed, disaggregated ultrasonically, and wet sieved at 2 mm and 250 µm. The 2 mm–250 µm fraction of each sample was dried at 60°C and weighed, and the abundance of the coarse-sand fraction was then calculated as a wt%. The coarse-sand fraction of each sample was next examined under a binocular microscope to determine what additional steps were needed (if any), on a sample-by-sample basis, to isolate the terrigenous, nonvolcanic material (the IRD) from the rest of the coarse-sand fraction. Physical separation techniques included hand picking and/or hydrochloric acid treatment to remove calcareous microfossils, hand picking of siliceous sponge spicules and pyritized burrows, and additional ultrasonic disaggregation and resieving to remove persistent “clayballs” in the coarse-sand fraction. Samples were reweighed after undergoing any of these additional treatments. Volcanic ash was generally not a significant component of the coarse-sand fraction; therefore, physical separation of the ash from the rest of the coarse-sand fraction by means of heavy liquid techniques was not performed. However, a minor correction was made to remove the estimated importance of ash in the IRD abundance calculation (wt%). This was done by assuming the density of ash to be 2.46 g/cm³ (Fisher, 1965; Huang et al., 1975), the density of the terrigenous, nonvolcanic fraction to be 2.65 g/cm³ (density of quartz), and the same grain volume (i.e., the same average grain size) for both grain types.

MARs are used in this study as the indicator of importance of IRD supply rather than IRD abundance (wt%), because IRD MARs are independent of the supply rates of other coarse sand-size components, such as volcanic ash and biogenic material. The MAR of the coarse sand-sized IRD was calculated as

$$\text{IRD MAR} = \text{CS\%} \times \text{IRD\%} \times \text{DBD} \times \text{LSR},$$

where IRD MAR is the mass accumulation rate (g/cm²/k.y.), CS% is the coarse-sand abundance (wt%), IRD% is the IRD abundance within the coarse-sand fraction (wt%), DBD is the dry-bulk density of the sediment (g/cm³), and LSR is the linear sedimentation rate (cm/k.y.). All values for these calculations are given in Table 1. Dry-

¹Larsen, H.C., Duncan, R.A., Allan, J.F., and Brooks, K. (Eds.), 1999. *Proc. ODP, Sci. Results*, 163: College Station, TX (Ocean Drilling Program).

²Department of Geological Sciences, Ohio State University, 125 S. Oval Mall, Columbus, OH 43210, U.S.A. (Present address: Department of Geology, Appalachian State University, Boone, NC, 28608, U.S.A.) stjohnke@appstate.edu

Table 1. Data used to calculate mass accumulation rates of coarse-sand ice-rafted debris, Site 918.

Core, section, interval (cm)	Depth (mbsf)	Calculated age (Ma)	CS (wt%)	IRD (wt%)	LSR (cm/k.y.)	DBD (g/cm ³)	MAR CS IRD (g/cm ² /k.y.)
163-918A-							
1H-1, 48–52	0.48	0.008	7.5	95.0	5.9	1.05	0.442
1H-1, 85–89	0.85	0.014	4.1	86.0	5.9	0.84	0.174
1H-2, 22–26	1.22	0.021	2.3	75.6	5.9	1.24	0.126
1H-2, 50–54	1.5	0.025	2.2	80.0	5.9	1.24	0.130
2H-1, 27–31	2.07	0.035	2.5	82.0	5.9	1.14	0.138
2H-1, 105–109	2.85	0.048	1.0	76.5	5.9	1.24	0.057
2H-2, 24–29	3.54	0.060	0.1	47.3	5.9	0.95	0.002
2H-2, 101–105	4.31	0.073	0.5	73.1	5.9	0.95	0.020
2H-3, 25–29	5.05	0.086	0.3	70.4	5.9	1.2	0.016
2H-4, 41–45	6.67	0.113	0.7	100.0	5.9	1.04	0.041

Notes: CS = coarse-sand abundance. IRD = IRD abundance within the coarse-sand fraction. LSR = average sedimentation rate. DBD = sediment dry bulk density. CS IRD MAR = mass accumulation rate of the coarse-sand IRD.

This is a sample of the table that appears on the volume CD-ROM.

Table 2. Composition estimates of the coarse-sand (250 μ m to 2 mm) ice-rafted debris, Site 918.

Core, section, interval (cm)	Depth (mbsf)	Calculated age (Ma)	0.250 mm–2 mm (%) quartz	C-g Acidic	F-g Mafic	C-g Mafic	Ultramafic	Sedimentary	Other
163-918A-									
1H-1, 48–52	0.48	0.008	71	7	13	0	2	6	0
1H-1, 85–89	0.85	0.014	87	1	8	3	0	1	0
1H-2, 22–26	1.22	0.021	80	18	0	0	0	0	2
1H-2, 50–54	1.5	0.025	66	29	3	0	1	1	1
2H-1, 27–31	2.07	0.035	79	8	5	2	1	2	2
2H-1, 105–109	2.85	0.048	71	21	3	0	0	4	3
2H-2, 24–29	3.54	0.060	85	3	10	0	0	2	0
2H-2, 101–105	4.31	0.073	81	11	0	1	0	1	5
2H-3, 25–29	5.05	0.086	85	9	0	5	0	1	0
2H-4, 41–45	6.67	0.113	91	4	0	1	0	0	3

This is a sample of the table that appears on the volume CD-ROM.

Table 3. Composition estimates of the >2-mm-size fraction ice-rafted debris, Site 918.

Core, section, interval (cm)	Depth (mbsf)	Calculated age (Ma)	>2 mm (%) quartz	C-g Acidic	F-g Mafic	C-g Mafic	Ultra-mafic	Sedimentary	Other
163A-918A-									
1H-1, 48–52	0.48	0.008	7.7	30.8	61.5	0.0	0.0	0.0	0.0
1H-1, 85–89	0.85	0.014	22.2	33.3	33.3	0.0	0.0	11.1	0.0
1H-2, 22–26	1.22	0.021	0.0	50.0	50.0	0.0	0.0	0.0	0.0
1H-2, 50–54	1.5	0.025	0.0	0.0	100.0	0.0	0.0	0.0	0.0
2H-1, 27–31	2.07	0.035	28.6	0.0	57.1	0.0	0.0	14.3	0.0
2H-1, 105–109	2.85	0.048	0.0	80.0	20.0	0.0	0.0	0.0	0.0
2H-2, 24–29	3.54	0.060							
2H-2, 101–105	4.31	0.073							
2H-3, 25–29	5.05	0.086							
2H-4, 41–45	6.67	0.113	0.0	0.0	0.0	100.0	0.0	0.0	0.0

This is a sample of the table that appears on the volume CD-ROM.

bulk density values were obtained from tables of discrete shipboard physical properties measurements in Shipboard Scientific Party (1994). The closest available discrete measurements were used as sample dry-bulk density values.

The general composition of the IRD was determined by random point counting 100 grains in each sample (or the total sample, if less than 100 grains were present) and classifying the grain types as either quartz, coarse-grained acidic, fine-grained mafic, coarse-grained mafic, ultramafic, sedimentary, or other. Compositions included in the other category include mica flakes, gypsum crystals, and unidentifiable grains. Composition estimates were made for both the 250- μ m to 2-mm size fraction (for which the IRD MARs were >0.0 g/cm²/

k.y.), and for the >2-mm size fraction, when present. Tables 2 and 3 list the compositions of the 250- μ m to 2-mm size fraction and the >2-mm size fraction, respectively, for each sample. Table 4 lists the component IRD MAR values calculated for the different grain compositions in the 250- μ m to 2-mm size fraction.

RESULTS

IRD abundances and MARs for each sample are listed in Table 1. IRD compositions of the 250- μ m to 2-mm size fraction and the >2-mm size fraction, are listed in Tables 2 and 3, respectively, for each

Table 4. Component IRD MAR calculated for the coarse-sand (250 μ m to 2 mm) ice-rafted debris composition categories, Site 918.

Core, section, interval (cm)	Depth (mbsf)	Calculated age (Ma)	MAR quartz (g/cm ² /k.y.)	MAR c-g acidic (g/cm ² /k.y.)	MAR f-g mafic (g/cm ² /k.y.)	MAR c-g mafic (g/cm ² /k.y.)	MAR ultramafic (g/cm ² /k.y.)	MAR sedimentary (g/cm ² /k.y.)	MAR other (g/cm ² /k.y.)
163-918A-									
1H-1, 48–52	0.48	0.008	0.314	0.031	0.057	0.000	0.009	0.027	0.000
1H-1, 85–89	0.85	0.014	0.152	0.002	0.014	0.005	0.000	0.002	0.000
1H-2, 22–26	1.22	0.021	0.101	0.023	0.000	0.000	0.000	0.000	0.003
1H-2, 50–54	1.50	0.025	0.086	0.038	0.004	0.000	0.001	0.001	0.001
2H-1, 27–31	2.07	0.035	0.109	0.011	0.007	0.003	0.001	0.003	0.003
2H-1, 105–109	2.85	0.048	0.041	0.012	0.002	0.000	0.000	0.002	0.002
2H-2, 24–29	3.54	0.060	0.002	0.000	0.000	0.000	0.000	0.000	0.000
2H-2, 101–105	4.31	0.073	0.016	0.002	0.000	0.000	0.000	0.000	0.001
2H-3, 25–29	5.05	0.086	0.013	0.001	0.000	0.001	0.000	0.000	0.000
2H-4, 41–45	6.67	0.113	0.037	0.002	0.000	0.000	0.000	0.000	0.001

This is a sample of the table that appears on the volume CD-ROM.

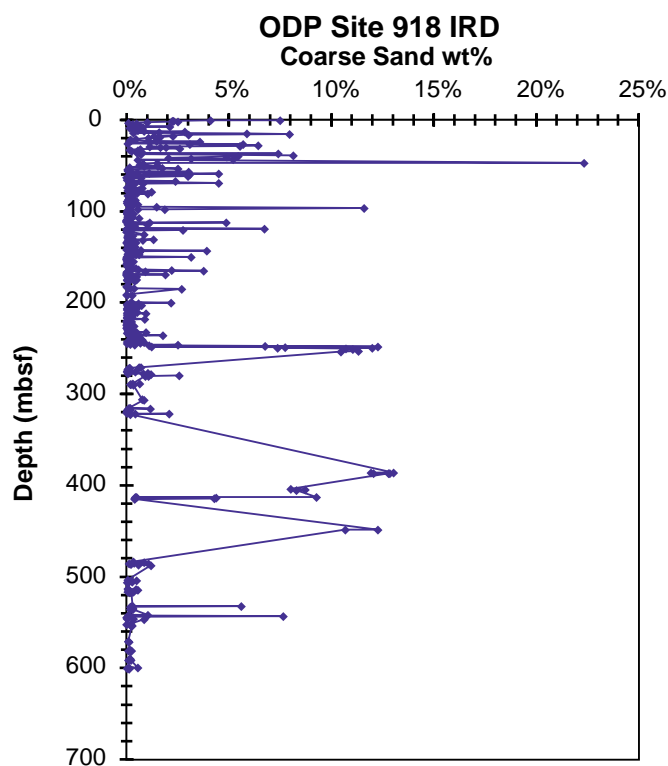


Figure 1. Abundance (wt%) of coarse sand-sized (250 μ m to 2 mm) IRD as a function of depth (mbsf).

sample. IRD MAR values calculated for the different grain compositions in the 250- μ m to 2-mm size fraction are given in Table 4.

IRD abundance (wt%) is plotted vs. depth downcore in Figure 1, and vs. calculated age in Figure 2. Figure 3 is a plot of IRD MAR vs. calculated age. Note the hiatus between ~1.7 and 1.4 Ma on the graphs.

ACKNOWLEDGMENTS

The author gratefully acknowledges Walter Hale and Alex Wuelbers at the Bremen Core Repository for their assistance with sampling, and Jessica Albrecht, Chris Brown, Rich Jacko, Maura Metheny, and Attiya Mobin-Uddin for their assistance with sample processing. Helpful and constructive reviews were provided by John Andrews and Gerard Bond. This work was funded by a JOI-USSSP postcruise research grant.

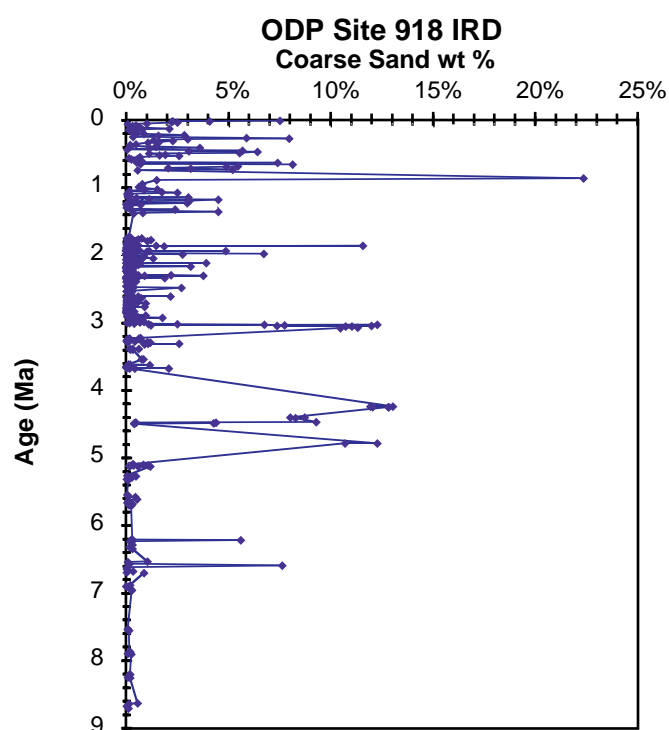


Figure 2. Abundance (wt%) of coarse sand-sized IRD as a function of sediment age (Ma).

REFERENCES

- Fisher, R.V., 1965. Settling velocity of glass shards. *Deep-Sea Res. Part A*, 12:345–353.
- Flower, B., 1998. Mid- to Late Quaternary stable isotope stratigraphy and paleoceanography at Site 919 on the southeast Greenland margin. In Saunders, A.D., Larsen, H.C., and Wise, S.W., Jr. (Eds.), *Proc. ODP, Sci. Results*, 152: College Station, TX (Ocean Drilling Program).
- Fukuma, K., 1998. Plio-Pleistocene magnetostratigraphy of sedimentary sequences from the Irminger Basin. In Saunders, A.D., Larsen, H.C., and Wise, S.W., Jr. (Eds.), *Proc. ODP, Sci. Results*, 152: College Station, TX (Ocean Drilling Program).
- Huang, T.C., Watkins, N.D., and Shaw, D.M., 1975. Atmospherically transported volcanic glass in deep-sea sediments: development of a separation and counting technique. *Deep-Sea Res.*, 22:185–196.
- Krissek, L.A., 1989. Late Cenozoic records of ice-rafting at ODP Sites 642, 643, and 644, Norwegian Sea: onset, chronology, and characteristics of glacial/interglacial fluctuations. In Eldholm, O., Thiede, J., Taylor, E., et al., *Proc. ODP, Sci. Results*, 104: College Station, TX (Ocean Drilling Program), 61–74.

- , 1995. Late Cenozoic ice-rafting records from Leg 145 sites in the North Pacific: late Miocene onset, late Pliocene intensification, and Pliocene–Pleistocene events. In Rea, D.K., Basov, I.A., Scholl, D.W., and Allan, J.F. (Eds.), *Proc. ODP, Sci. Results*, 145: College Station, TX (Ocean Drilling Program), 179–194.
- Krissek, L.A., Morley, J.J., and Lofland, D.K., 1985. The occurrence, abundance, and composition of ice-rafted debris in sediments from Deep Sea Drilling Project Sites 579 and 580, northwest Pacific. In Heath, G.R., Burckle, L.H., et al., *Init. Repts. DSDP*, 86: Washington (U.S. Govt. Printing Office), 647–655.
- Larsen, H.C., Saunders, A.D., Clift, P.D., Beget, J., Wei, W., Spezzaferri, S., and the ODP Leg 152 Scientific Party, 1994. Seven million years of glaciation in Greenland. *Science*, 264:952–955.
- Shipboard Scientific Party, 1994. Site 918. In Larsen, H.C., Saunders, A.D., Clift, P.D., et al., *Proc. ODP, Init. Repts.*, 152: College Station, TX (Ocean Drilling Program), 177–256.
- Spezzaferri, S., 1998. Planktonic foraminifer biostratigraphy and paleoenvironmental implications of Leg 152 Sites (East Greenland Margin). In Saunders, A.D., Larsen, H.C., and Wise, S.W., Jr. (Eds.), *Proc. ODP, Sci. Results*, 152: College Station, TX (Ocean Drilling Program).
- von Huene, R., Crouch, J., and Larson, E., 1976. Glacial advance in the Gulf of Alaska area implied by ice-rafted material. In Cline, R.M., and Hays, J.D. (Eds.), *Investigation of Late Quaternary Paleoceanography and Paleoclimatology*. Mem.—Geol. Soc. Am., 145:411–422.
- von Huene, R., Larson, E., and Crouch, J., 1973. Preliminary study of ice-rafted erratics as indicators of glacial advances in the Gulf of Alaska. In Kulm, L.D., von Huene, R., et al., *Init. Repts. DSDP*, 18: Washington (U.S. Govt. Printing Office), 835–842.
- Wei, W., 1998. Calcareous nannofossils from Leg 152 on the southeast Greenland margin. In Saunders, A.D., Larsen, H.C., and Wise, S.W., Jr. (Eds.), *Proc. ODP, Sci. Results*, 152: College Station, TX (Ocean Drilling Program).

Date of initial receipt: 5 January 1998

Date of acceptance: 15 May 1998

Ms 163SR-119

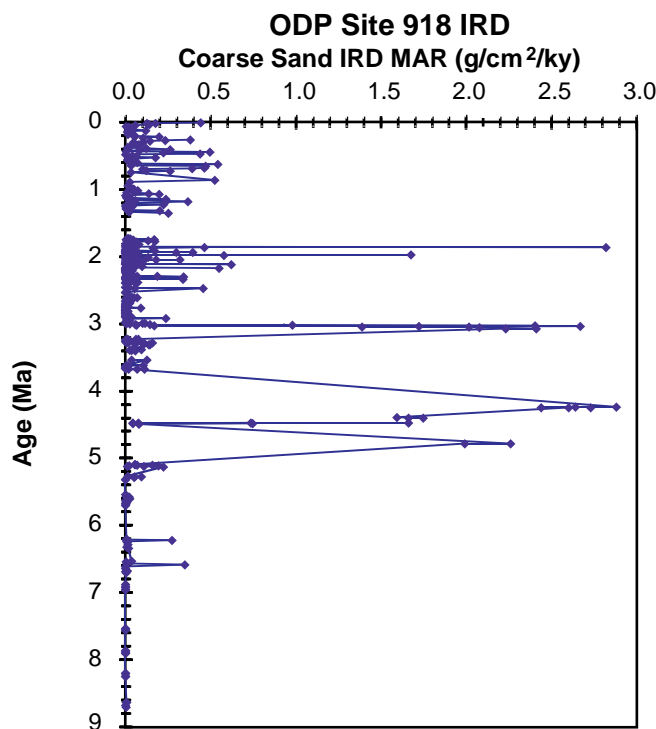


Figure 3. Mass accumulation rate of the coarse sand-sized IRD as a function of sediment age (Ma).